Parton energy loss limits and shadowing in Drell-Yan dimuon production

M.A. Vasiliev[i*], M.E. Beddo[g], C.N. Brown[c], T.A. Carey[f], T.H. Chang[g†], W.E. Cooper[c], C.A. Gagliardi[i], G.T. Garvey[f], D.F. Geesaman[b], E.A. Hawker[i,f], X.C. He[d], L.D. Isenhower[a], D.M. Kaplan[e], S.B. Kaufman[b], D.D. Koetke[j], W.M. Lee[d], M.J. Leitch[f], P.L. McGaughey[f], J.M. Moss[f], B.A. Mueller[b], V. Papavassiliou[g], J.C. Peng[f], G. Petitt[d], P.E. Reimer[f,b], M.E. Sadler[a], W.E. Sondheim[f], P.W. Stankus[h], R.S. Towell[a,f], R.E. Tribble[i], J.C. Webb[g], J.L. Willis[a], G.R. Young[h]

(FNAL E866/NuSea Collaboration)

[a] *Abilene Christian University, Abilene, TX 79699*

[b] *Argonne National Laboratory, Argonne, IL 60439*

[c] *Fermi National Accelerator Laboratory, Batavia, IL 60510*

[d] *Georgia State University, Atlanta, GA 30303*

[e] *Illinois Institute of Technology, Chicago, IL 60616*

[f] *Los Alamos National Laboratory, Los Alamos, NM 87545*

[g] *New Mexico State University, Las Cruces, NM, 88003*

[h] *Oak Ridge National Laboratory, Oak Ridge, TN 37831*

[i] *Texas A & M University, College Station, TX 77843*

[j] *Valparaiso University, Valparaiso, IN 46383*

(August 5, 1999)

A precise measurement of the ratios of the Drell-Yan cross section per nucleon for an 800 GeV/c proton beam incident on Be, Fe and W targets is reported. The behavior of the Drell-Yan ratios at small target-parton momentum fraction is well described by an existing fit to the shadowing observed in deep-inelastic scattering. The cross-section ratios as a function of the incident-parton momentum fraction set tight limits on the energy loss of quarks passing through a cold nucleus.

24.85.+p; 13.85.Qk; 25.40.Ve

The Drell-Yan process can be used to study the interactions of fast partons traversing cold nuclei. Only initial-state interactions are important in Drell-Yan since the dimuon in the final state does not interact strongly with the partons in the medium. This makes Drell-Yan scattering an ideal tool to study energy loss of fast quarks in nuclear matter – a subject of considerable theoretical interest [1–4] with significant implications for the physics of relativisitic heavy-ion collisions – by comparing the observed yields from a range of nuclear targets.

Drell-Yan scattering is closely related to deep-inelastic scattering (DIS) of leptons, but unlike DIS it is directly sensitive to antiquark contributions in target parton distributions. When DIS on nuclei occurs at $x < 0.08$, where x is the parton momentum fraction, the cross section per nucleon decreases with increasing nucleon number A due to shadowing [5,6]. Shadowing should also occur in Drell-Yan dimuon production at small x_2, the momentum fraction of the target parton, and theoretical calculations indicate that shadowing in the two reactions has a common origin [7–9]. This should be particularly apparent at $x < 0.06$ where DIS on nuclei, like Drell-Yan, is dominated by scattering off sea quarks.

Fermilab Experiment 866 (E866) measured the nuclear dependence of Drell-Yan dimuon production by 800 GeV/c protons on Be, Fe and W targets at larger values of x_1, the momentum fraction of the beam parton, larger values of x_F ($\approx x_1 - x_2$), and smaller values of x_2 than reached by the previous experiment, Fermilab E772 [10]. The extended kinematic coverage of E866 significantly increases its sensitivity to parton energy loss and shadowing. This Letter reports the results.

The experiment used the same 3-dipole magnetic spectrometer that was described in [11]. An 800 GeV/c extracted proton beam averaging 3×10^{11} protons per 20 s spill bombarded one of three solid targets or an empty target frame. The Be, Fe and W targets were 9.4% – 19% of an interaction length thick, with relative thicknesses chosen to match the background singles rates present in the spectrometer detectors. The targets were placed at the same z location far upstream of the main dipole magnet to optimize the acceptance at low x_2 and large x_F. During a cycle, 2 beam spills were taken on each target and 1 spill was collected on an empty location. The non-interacting beam was intercepted by a copper beam dump, which was followed by a thick absorber that removed hadrons produced in the target and the dump. This ensured that only muons traversed the four tracking stations. The trigger required a pair of triple-hodoscope coincidences having the topology of a muon pair from the target. Typically 1400 triggers per second were recorded with an average live time of 93%.

Over 130,000 muon pairs with dimuon mass in the range $4.0 < M < 8.4$ GeV/c^2 survived analysis cuts. Random pairs were subtracted from the data using simulated opposite-charge random dimuons constructed by mixing single-muon tracks that were obtained simultaneously from prescaled single-muon triggers. The normal-

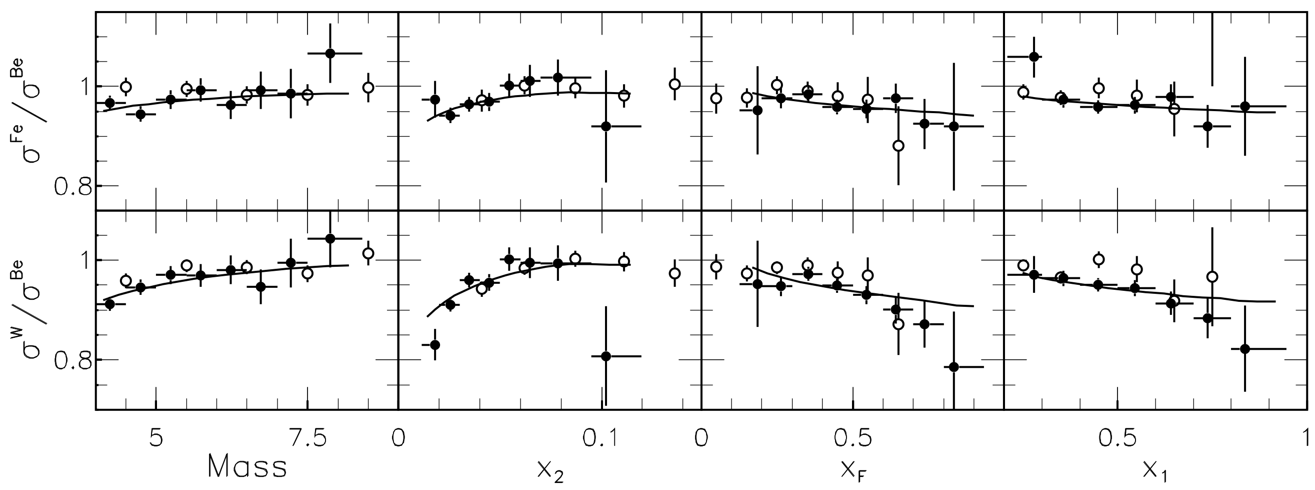

FIG. 1. Ratios of the measured cross section per nucleon for Drell-Yan events versus dimuon mass (in GeV/c^2), x_2, x_F and x_1. The upper (lower) panels show ratios of Fe/Be (W/Be) from the present experiment as solid circles and Fe/C (W/C) from E772 as open circles. The errors are statistical only. The solid curves are the predicted cross-section ratios for the present experiment, integrated over the hidden variables, from leading-order calculations using EKS98 [12] and MRST [13].

ization factor for the random correction was evaluated by comparing to the observed rate of same-charge muon pairs in the data, whose kinematic distributions agreed well with those of the simulated same-charge muon pairs. The random rate was 9% of the real events, and it occurred primarily at low dimuon mass and high p_T. A residual 3% background from the empty target was also subtracted. The overall systematic normalization uncertainty in the cross-section ratios reported here is 1%.

The Drell-Yan events obtained by E866 extend over the ranges $0.01 < x_2 < 0.12$ and $0.21 < x_1 < 0.95$, with $\langle x_2 \rangle = 0.038$ and $\langle x_1 \rangle = 0.46$. They cover the range $0.13 < x_F < 0.93$ and provide good p_T coverage to 4 GeV/c. Ratios of the cross section per nucleon for Fe to Be and W to Be versus dimuon mass, x_2, x_F and x_1 are shown in Fig. 1, along with similar results from E772 for Fe to C and W to C. The figure shows very good agreement between the experiments for the cross section ratios versus x_2. The agreement versus other variables is also reasonable, given the much smaller $\langle x_2 \rangle$ and, hence, increased shadowing of the present data. (The A dependence observed here and in E772 implies the change in the cross-section ratios due to the choice of Be vs. C is small compared to the effect of the difference in $\langle x_2 \rangle$.) The reduction in the cross section per nucleon on the heavy targets, characteristic of shadowing, is apparent at small x_2. A similar reduction, part of which could be related to incident-parton energy loss, is apparent at large x_F and x_1. However, it is important to recognize that the spectrometer acceptance coupled to the intrinsic Drell-Yan cross section leads to a strong anti-correlation between x_2 and x_F for the observed events. Therefore, the events that show the cross-section reduction at large x_F and x_1 are in general the same events that appear in the shadowing region.

To identify the contributions from shadowing, Fig. 1 also shows the predicted cross-section ratios, integrated over the hidden variables, from leading-order Drell-Yan calculations using the code EKS98 [12] together with the MRST parton distribution functions [13]. Similar results are obtained using CTEQ5M or CTEQ5L parton distributions [14]. EKS98 describes the ratios $f_A(x,Q^2)/f_p(x,Q^2)$ of the various quark flavors in nucleus A, compared to those in the proton. It has been tuned to fit the shadowing observed in DIS [15] and E772 while conserving baryon number and momentum. EKS98 provides an unbiased way to separate the effects of shadowing and energy loss in the present data because it uses a single shadowing function to describe the nuclear dependence of all sea quark distributions at its initial scale ${Q_0}^2 = 2.25$ GeV^2 and only DIS results are used to constrain that function for $x \lesssim 0.1$.

The shape and magnitude of the ratios versus x_2 are well reproduced by the shadowing predictions. Most of the A dependence observed in the ratios versus mass, x_F and x_1 is also explained by shadowing at small x_2. As a further test of the shadowing parametrization, Fig. 2 shows the W/Be ratios vs. x_1, with the events separated into two subsets at the median x_2 value. This eliminates the correlation in acceptance between x_1 and x_2 for the large x_2 subset of the data, indicated by the flat shadowing prediction, and substantially reduces the correlation for the small x_2 subset, indicated by the reduced slope of the shadowing prediction compared to Fig. 1. The cross-section ratios differ by several percent when events at the same x_1 are observed in the two subsets of the

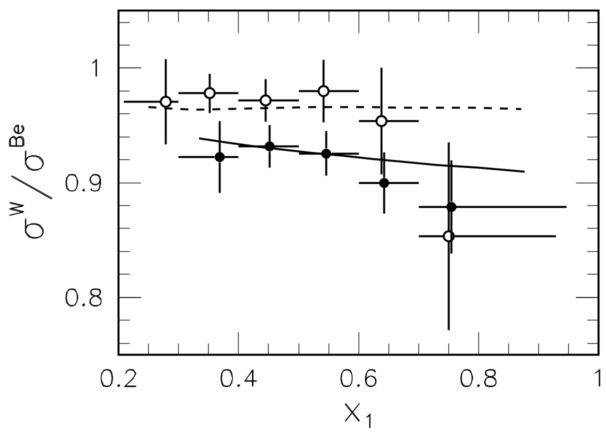

FIG. 2. Ratios of the measured Drell-Yan cross section per nucleon for W/Be versus x_1. The solid (open) circles are those events with x_2 less than (greater than) 0.036, and the solid (dashed) curve is the corresponding shadowing prediction.

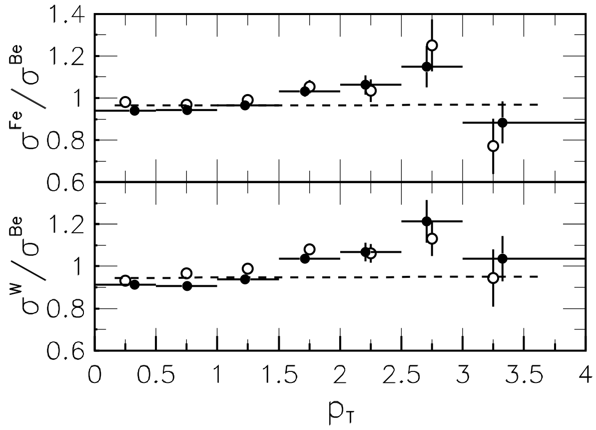

FIG. 3. Ratios of the measured Drell-Yan cross section per nucleon versus p_T. Solid circles show ratios of Fe/Be and W/Be from the present experiment, and open circles show ratios of Fe/C and W/C from E772. The dashed curves are shadowing predictions for the present experiment.

data. EKS98 describes these differences well with no free parameters. Similar results are obtained when examining the mass or x_F dependence. This is the first experimental demonstration that the shadowing observed in Drell-Yan and DIS is quantitatively similar.

Figure 3 shows the measured ratios of the Drell-Yan cross section per nucleon as a function of p_T. Unlike the longitudinal variables that have strongly correlated acceptances, the p_T acceptance in E866 is nearly independent of the other kinematic variables, so the shadowing calculations predict constant cross-section ratios, as shown in the figure. The data demonstrate a clear p_T dependence however. The slight reduction in the cross section per nucleon observed for heavy nuclei at small p_T, coupled with the increase in the cross section per nucleon at large p_T, is characteristic of multiple scattering of the incident partons as they traverse the nucleus. But the apparent drop in the cross section per nucleon on the heavy targets for $p_T > 3$ GeV/c does not fit this model.

The x_1 dependence of the cross-section ratios provides the best direct measure of the energy loss of the incident quarks in the nuclear medium. Table I gives the ratios of the measured cross section per nucleon as a function of x_1 and the mean values of x_1 and x_2 for each bin. However, as shown above, shadowing at small x_2 explains a substantial fraction of the apparent variation in the cross-section ratios versus x_1. This must be removed before one can isolate a nuclear dependence due to energy loss. Figure 4 and Table I show the cross-section ratios vs. x_1, corrected for shadowing by weighting each event with the calculated ratio of the Drell-Yan cross sections per nucleon for deuterium and nucleus A at the same (x_1, x_2, Q^2), using EKS98 and MRST.

Several groups have studied energy loss of partons in nuclei. Their results can be expressed in terms of the average change in the incident-parton momentum fraction, Δx_1, as a function of target A. Gavin and Milana [1] analyzed the E772 Drell-Yan data for energy loss based on the parametrization

$$\Delta x_1 = -\kappa_1 \, x_1 \, A^{1/3}, \tag{1}$$

where the factor κ_1 may have a Q^2 dependence. They based the form (1) on an analogy to the transverse spin asymmetry in direct photon production. From a comparison to the x_F dependence seen by E772 and neglecting shadowing, they concluded that the fractional energy loss of quarks passing through nuclei is $\approx 0.4\%$/fm. Recently, other groups have assumed equivalent formulations with even more rapid energy loss [16,17]. Brodsky and Hoyer [2] argued that the energy loss found by Gavin and Milana was too large since the time scale for QCD bremsstrahlung was too short to allow for multiple contributions to the energy loss. Brodsky and Hoyer used an analogy to the photon bremsstrahlung process to obtain

TABLE I. Ratios of the cross section per nucleon for Fe to Be and W to Be as functions of x_1, as measured and corrected for shadowing. Also given are mean values of x_1 and x_2 for each bin. $\langle x_F \rangle = \langle x_1 \rangle - \langle x_2 \rangle$, and $\langle M^2 \rangle = \langle x_1 \rangle \langle x_2 \rangle s$. The errors are statistical only.

			Measured		Corrected	
Range	$\langle x_1 \rangle$	$\langle x_2 \rangle$	$\sigma^{\mathrm{Fe}}/\sigma^{\mathrm{Be}}$	$\sigma^{\mathrm{W}}/\sigma^{\mathrm{Be}}$	$\sigma^{\mathrm{Fe}}/\sigma^{\mathrm{Be}}$	$\sigma^{\mathrm{W}}/\sigma^{\mathrm{Be}}$
-0.3	0.279	0.055	1.059(41)	0.971(37)	1.085(42)	1.004(39)
0.3-0.4	0.356	0.046	0.973(16)	0.964(15)	1.004(16)	1.007(16)
0.4-0.5	0.448	0.039	0.959(14)	0.951(13)	0.994(14)	1.004(14)
0.5-0.6	0.545	0.034	0.962(17)	0.944(16)	1.002(17)	1.005(17)
0.6-0.7	0.642	0.030	0.979(25)	0.914(23)	1.024(26)	0.980(25)
0.7-0.8	0.738	0.026	0.920(42)	0.884(40)	0.967(45)	0.955(44)
0.8-	0.836	0.023	0.960(99)	0.822(86)	1.01(10)	0.894(94)

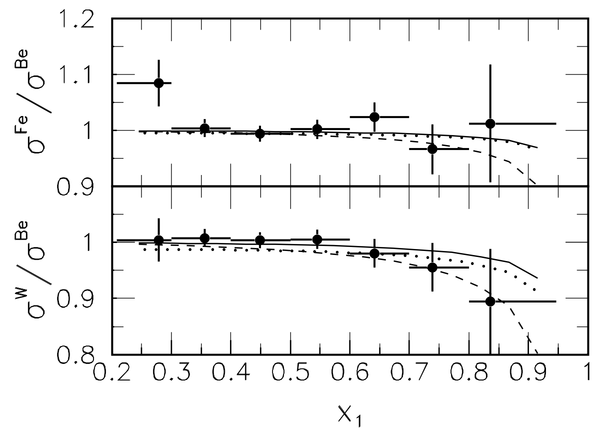

FIG. 4. Ratios of the cross section per nucleon versus x_1 for Fe/Be (upper panel) and W/Be (lower panel), corrected for shadowing. The solid curves are the best fit using the energy loss form (1), and the dashed curves show the 1σ upper limits. The dotted curves show the 1σ upper limits using the energy loss form (3). The 1σ upper limit curves using the energy loss form (2) are essentially identical to those using form (3).

a form for gluon radiation leading to an initial-parton energy loss [18]

$$\Delta x_1 \approx -\frac{\kappa_2}{s} A^{1/3}, \tag{2}$$

where s is the square of the nucleon-nucleon center-of-mass energy. They found an upper limit for the gluon radiation from the uncertainty relation. They also noted that elastic scattering should make a similar contribution to the energy loss. Overall, they concluded that energetic partons should lose $\lesssim 0.5$ GeV/fm in nuclei. The formulation developed by Brodsky and Hoyer was extended by Baier *et al.* [3,4]. They found that the energy loss of sufficiently energetic partons depends on a characteristic length and the broadening of the squared transverse momentum of the parton. For finite nuclei, both factors vary as $A^{1/3}$, so Baier *et al.* predict

$$\Delta x_1 \approx -\frac{\kappa_3}{s} A^{2/3}. \tag{3}$$

Baier *et al.* also predict that energy loss may be different in hot and cold nuclear matter and that there could a large coherent effect in relativistic heavy-ion collisions. In contrast, tight limits have been placed on energy loss in S+S and Pb+Pb collisions [19], but the parton momenta relative to the hadronic medium were very much smaller in those cases than in the present experiment, making a direct comparison difficult.

Given these energy loss expressions, it is possible to obtain empirical values for the κ's by performing simultaneous fits to the Fe/Be and W/Be Drell-Yan cross-section ratios versus x_1 in Fig. 4. We assume that κ_1 is Q^2-independent [1,2] when using form (1) and that our incident quarks are sufficiently energetic when using form (3). Curves corresponding to the fits are included in Fig. 4. When assuming the form (1), we find $\kappa_1 = 0.0004\pm0.0009$. This implies that the observed fractional energy loss of the incident quarks is $< 0.14\%$/fm at 1σ. For the energy loss forms (2) and (3), the best fits imply essentially zero energy loss. We find the 1σ upper limits to be $\kappa_2 < 0.75$ GeV^2 and $\kappa_3 < 0.10$ GeV^2. The κ_2 limit indicates that the incident quarks lose energy at a constant rate of < 0.44 GeV/fm. The κ_3 limit implies that the observed energy loss of the incident quarks within the model of Baier *et al.* is $\Delta E < 0.046$ GeV/fm^2 $\times\ L^2$, where L is the quark propagation length through the nucleus. This is very close to the lower value given by Baier *et al.* for cold nuclear matter [20]. In all three cases, the quoted errors include both statistics and the overall normalization uncertainty, with the latter dominating.

In summary, this Letter reports a measurement of the ratios of the Drell-Yan cross section per nucleon for Fe to Be and W to Be. Nuclear shadowing is found to be important in the small x_2 domain, where the shadowing observed in Drell-Yan has been demonstrated to be quantitatively similar to that in DIS. The cross-section ratios versus x_1 provide direct upper limits on the energy loss of the incoming parton as it traverses a cold nucleus that are tighter than previous constraints. Shadowing and initial-state energy loss are processes that occur in both Drell-Yan production and J/ψ formation. Hence, these results should also further the understanding of J/ψ production, which is required if it is to be used as a signal for the quark-gluon plasma in relativistic heavy-ion collisions.

We thank R. Vogt for many useful discussions and the Fermilab Particle Physics, Beams and Computing Divisions for their assistance. This work was supported in part by the U.S. Department of Energy.

* On leave from Kurchatov Institute, Moscow, Russia.
† Present address: University of Illinois, Urbana, IL 61801.

[1] S. Gavin and J. Milana, Phys. Rev. Lett. **68**, 1834 (1992).
[2] S.J. Brodsky and P. Hoyer, Phys. Lett. B **298**, 165 (1993).
[3] R. Baier *et al.*, Nucl. Phys. B **484**, 265 (1997).
[4] R. Baier *et al.*, hep-ph/9804212.
[5] D.F. Geesaman, K. Saito and A.W. Thomas, Ann. Rev. Nucl. Part. Sci. **45**, 337 (1995).
[6] M. Arneodo *et al.*, Nucl. Phys. B **441**, 3 (1995).
[7] L.L. Frankfurt, M.I. Strikman and S. Liuti, Phys. Rev. Lett. **65**, 1725 (1990).
[8] B. Kopeliovich, Proc. Workshop Hirschegg '95, ed. by H. Feldmeier and W. Norenberg, Darmstadt, 1995, 102, hep-ph/9609385.

[9] S.J. Brodsky, A. Hebecker and E. Quack, Phys. Rev. D **55**, 2584 (1997).
[10] D.M. Alde *et al.*, Phys. Rev. Lett. **64**, 2479 (1990).
[11] E. Hawker *et al.*, Phys. Rev. Lett. **80**, 3715 (1998).
[12] K.J. Eskola, V.J. Kolhinen and P.V. Ruuskanen, Nucl. Phys. B **535**, 351 (1998); K.J. Eskola, V.J. Kolhinen and C.A. Salgado, hep-ph/9807297.
[13] A.D. Martin *et al.*, Eur. Phys. J. C **4**, 463 (1998).
[14] H.L. Lai *et al.*, hep-ph/9903282.
[15] M. Arneodo *et al.*, Nucl. Phys. B **481**, 3 (1996); Nucl. Phys. B **481**, 23 (1996).
[16] C. Gale, S. Jeon and J. Kapusta, Phys. Rev. Lett. **82**, 1636 (1999).
[17] E. Marco and E. Oset, Nucl. Phys. A **645**, 303 (1999).
[18] Eq. 2 and Eq. 7 of [2] differ because we define $\Delta x_1 = \Delta E_{parton}/E_{beam}$. Eq. 7 of [2] uses $\Delta x_1 = \Delta E_{parton}/E_{parton}$. S.J. Brodsky, private communication (1999).
[19] X.-N. Wang, Phys. Rev. Lett. **81**, 2655 (1998).
[20] Note that [4] indicates that the estimate 0.02 GeV/fm^2 given in [3] should be increased by a factor of 2.